Proceedings of the ASME 2018 37th International Conference on Ocean, Offshore and Arctic Engineering
OMAE2018
June 17-22, 2018, Madrid, Spain

OMAE2018-78372

CFD Simulations of Helical Strakes Reducing Vortex Induced Motion of a Semi-Submersible

Jiawei He
Collaborative Innovation Center for Advanced Ship and Deep-Sea Exploration, State Key Laboratory of Ocean Engineering, School of Naval Architecture, Ocean and Civil Engineering, Shanghai Jiao Tong University, Shanghai 200240, China

Decheng Wan*
Collaborative Innovation Center for Advanced Ship and Deep-Sea Exploration, State Key Laboratory of Ocean Engineering, School of Naval Architecture, Ocean and Civil Engineering, Shanghai Jiao Tong University, Shanghai 200240, China
*Corresponding author: dcwan@sjtu.edu.cn

Zhiqiang Hu
School of Marine Science and Technology, Newcastle University, Newcastle upon Tyne, NE1 7RU, UK

ABSTRACT

This paper describes a set of VIM CFD simulations for a semi-submersible with and without helical strakes. The numerical investigations are conducted under low Reynolds number(*Re*) using naoe-FOAM-SJTU, a solver developed based on the open source framework OpenFOAM. The self-developed six degree-of-freedom (6DoF) motion module and mooring system module are applied to model motions of semi-submersible and the constraint of mooring lines, respectively. To carry out the calculations, turbulence closure has been chosen the Shear Stress Transport (SST) based Delay Detached eddy simulation (DDES), which uses the RANS model inside the boundary region and LES model outside the boundary area. This allows a realistic simulation within the boundary region where the vortex shedding is taking place, while not using unnecessary amounts of computational power. The Vortex Induced Motion(VIM) of semi-submersible with and without helical strakes was compared against each other for different reduced velocities (*Ur*). The flow characteristics of the semi-submersible platform is studied based on the characteristics of vortex shedding. For different current incident angles, time histories, trajectories and vorticity of the semi-submersible at different reduced velocities are reported. The result shows our CFD solver naoe-FOAM-SJTU is applicable and reliable to study VIM of semi-submersibles.

Keywords: Vortex-induced motion; Semi-submersible; CFD; Helical strakes.

INTRODUCTION

Vortex-Induced Motion (VIM), which occurs as a consequence of exposure to strong current such as Loop Current eddies in the Gulf of Mexico, is a common phenomenon on varies kinds of deep-draft offshore platforms such as semi-submersible and Spar. As a result of the increased draft, the semi-submersibles are susceptible to coherent vortex shedding, and the VIM increases significantly. The geometry of semi-submersibles, multi- column and multi-pontoon, implies a more complex VIM phenomenon than that of Spar platforms[1].

The VIM response of semi-submersible platforms can have a significant impact on the mooring and riser components, results in fatigue. As Chen et al. [2] pointed out, the field measurements of VIM of offshore floaters are rarely acquired. So the scaled model testing is currently the most used when determining VIM for offshore platform design. Nevertheless, scaled model tests are limited in their ability to represent the full-scale Reynolds number and also cannot fully represent waves effects, nonlinear mooring system behavior. Xiang, et al.[3] estimated the damage caused by the VIM in the fatigue life of risers and mooring systems, for the Deep Draft Semi-submersible platform, and pointed out the fatigue life estimates based on the model test observations are considered to be conservative. When Kara et al. (2016) [4] study for deep draft column stabilized floaters' VIM phenomenon, he found that the CFD approach can be a cost effective and reliable alternative to model testing, which is costly

and schedule constrained making it impractical in the early phase of a project.

With use of CFD, Rijken (2014) [5] investigated the VIM responses of the semi-submersibles with three different column cross-sectional shapes, including square, rectangular and five-sided shapes. Waals et al. (2007)[6] discussed the effect of mass ratio and draft on VIM of semi-submersible platform, and found that the semi-submersible with smaller column height showed much less flow induced cross-flow and yaw response than that with larger column height. Gonçalves et al. discussed the effects of current incidence angles, hull appendages,[7] surface waves, external damping and draft conditions[8] to study the VIM of a semi-submersible platform systematically. Chen et al. (2016) [9] used the Finite-Analytic Navier–Stokes (FANS) code in conjunction with a moving overset grid approach to simulate vortex-induced motions (VIM) of a deep draft semi-submersible. A DES calculation is performed to check against the LES model. Antony et al. [10] utilizes computational fluid dynamics (CFD) analysis and model testing to determine the sensitivity of VIM responses of deep draft column stabilized floaters (DDCSF) to geometric parameters. The CFD tools used in his study are AcuSolve™ from Altair Engineering, Fluent™ from ANSYS and STAR-CCM+™from CD-adapco. Kara et al. (2016) [4] used OpenFOAM on a model scale, deep draft, "Paired-Column" semi-submersible to estimate the VIM response, and proposed that DES was a powerful turbulence model and recommended for CFD based VIM simulations.

If there is no suppression devices were taken to the semi-submersible, it will bring serious influence to the platforms with VIM. To mitigate the influence of VIM, the industry has applied a tried suppression device: helical strakes. Helical strakes can destroy regular vortex shedding in the inline direction and prevent shedding from becoming correlated in the cross-flow direction [11].While helical strakes are known to work on cylindrical structures, such as flexible risers and Spars. Historically, when used offshore in the design of spar-platforms, and is shown to be extremely efficient. The helical strakes are very effective in suppressing the vortex shedding from circular cylinders and can reduce the strength of vortex shedding by up to 99%[12]. The problem with semi-submersibles is that the outside of the hull is littered with appurtenances: anodes, mooring lines, etc. what's more, the column of the semi-submersibles sometimes is the rectangle. These items have been found to negate the effectiveness of strakes due to their effect on the fluid boundary layer around the semi-submersible. One method of altering the geometry is welding the helical strakes on the round corner of the semi-submersible. Therefore, plenty of research work are being done in this field. Holland et al., (2017)[13] numerically investigated the helical strakes are attached to the geometry to break up the coherence of the vortex shedding and the performance of these strakes. The computations of semi-submersible are carried out in full-scale with the CFD tool of STAR-CCM+™. Xu et al., (2012)[14] studied VIM response of a semisubmersible with helical strakes by model test and Computational Fluid Dynamics (CFD) with AcuSolve™.The model test was performed in the towing tank of FORCE Technologies in Copenhagen, Denmark in Dec, 2010. Both the model test and CFD analysis demonstrated that the max RMS value of simulated *A/D* of VIM responses reduced more than 20%, which compared with an equivalent conventional semisubmersible without installed helical strakes.

As mentioned by Kim et al. [15]Published model test data for simplified semi-submersible models and for multi-column floating platforms show that the maximum VIM response amplitude can reach slightly more than half the column diameter in both cases.

As a numerical method in CFD, detached eddy simulation (DES) has been widely used to simulate the separated flow in VIM, due to the acceptable accuracy and reasonable computational cost. DES combines the favorable aspects of RANS that is efficient and accurate at attached boundary layers and of LES which is more accurate in highly separated flows. Tan et al.(2013) [16] used DES to compute the VIM of a multi-column platform in different loading conditions. The DES turbulence model proves to be have provided very good agreement with results in the tow test.

The main objective of the present study is to investigate the VIM of a semi-submersible with multi-column, and the effects of the column with helical strakes on VIM are also investigated. The characteristics of VIM over different reduced velocities are also analyzed. Free-surface motion is ignored in this study.

NUMERICAL SETUP AND COMPUTATION'S DETAILS

Semi-submersible Model and Grid System

The computational dimensions of semi-submersible model in this paper were taken from Waals et al.(2007)[6] and Chen et al.(2015)[2]. The present computation of the semi-submersible was welding the helical strakes on the round corner of columns. Main dimensions of the semi-submersible platform are shown in the Table 1 and Figure 1.

TABLE 1 Main dimensions of the semi-submersible platform

Description	Symbol	Unit	Full-scale	Model-scale
Scale ratio	-	-	1:1	1：70
Length between columns	*S*	m	56	0.8
Draft	*T*	m	35	0.5
Column width	*L*	m	14	0.2
Column round corner	*R*	m	2.2	0.0314
Pontoon height	*P*	m	10.5	0.15
Displacement	Δ	*tons*	53000	0.155
Mass	*M*	*tons*	44000	0.128

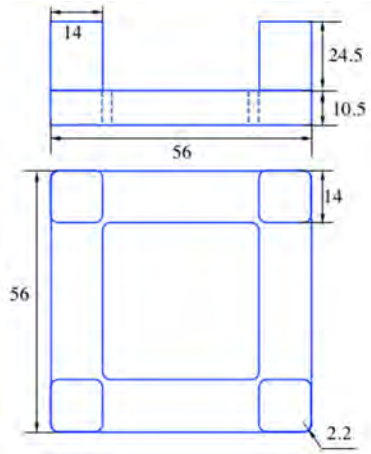

FIGURE 1. Main dimensions of a semi-submersible platform with the columns are rectangle in cross section with edges smoothed.

The helical strakes attached to the columns for simulations use dimensions taken from spar-platforms, which is the same with Holland, V. et al. (2017) [13]investigated helical strakes as a means of reducing the vortex induced forces on a semi-submersible. The width of the strakes was calculated to be 13% of the column width (0.13×0.2=0.026m). Fig. 2 shows the four identical columns with a helical strake covering each round corner. It is worth noting that in this study the helical strakes were placed at the rounded column corners as this is the site where significant vortex shedding occurs.

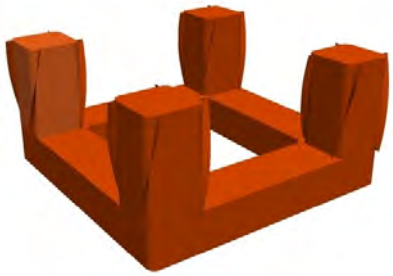

FIGURE 2. The four columns of semi-submersible with helical strakes.

Table 2 presents the simulation cases of this study. All numbers are in model scale (1:70). The current speeds considered are reasonably low thus neglecting the wave effects should not cause significant errors in the solution. wave drag may begin to have a non-negligible effect at this speed. The Reynolds numbers involved are between 1.36×10^4 and3.39×10^4. The length scale D =0.2(the length of column) used to determine the Re number.

TABLE 2. CFD simulation case conditions of the semi-submersible model

Helical strakes	Reduced velocity U_r	Flow velocity (m/s)	*Re*
without strakes	8	0.0680	1.36×10^4
	11	0.0905	1.81×10^4
	20	0.1697	3.39×10^4
with strakes	8	0.0680	1.36×10^4
	11	0.0905	1.81×10^4
	20	0.1697	3.39×10^4

Here, the reduced velocity (U_r) is normally defined as:

$$U_r = \frac{U}{f_n D} \quad (1)$$

where U is the current velocity, f_n is the natural frequency of the motion in the cross-flow direction in calm water, and D is the characteristic length of the structure normal to the current.

The self-developed six degree-of-freedom (6DoF) motion module and linear springs system module are applied to model motions of semi-submersible and the constraint of mooring lines, respectively.

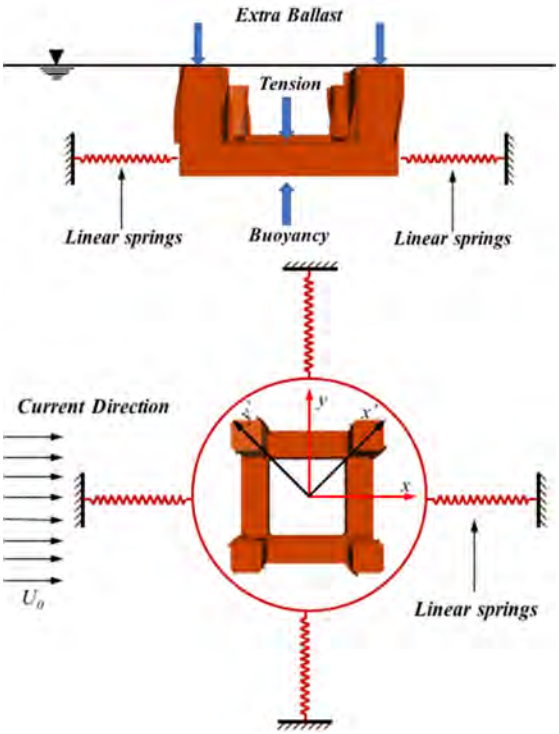

FIGURE 3. Definitions of current incidence angles, spring system and columns with helical strakes.

Computational Domain and Grids

The computational domain shows as the Figure 4, the size of which is $12B \times 6B \times 3T$ (length × width × depth), where B is the hull width and T is the draft of the semi-submersible. The computational domain extends to capture the wake, the mesh regions were refined locally. The outer, far-field region has a coarser mesh while the inner wake zone has finer mesh. Detail of the refinement zone around the semi-submersible and helical strakes is shown in Figure 5. The total grid number for the simulation is around 5.6 million. The time step is 0.01 s in each case. The workload is distributed into 40 processors on a Linux cluster for calculation. Motion of the rigid body is captured via Arbitrary Lagrangian-Eulerian (ALE). The naoe-FOAM-SJTU uses an ALE method to handle rigid body motion of the semi-submersible. A uniform flow, $u_x = U_0,\ u_y = u_z = 0$, was set at the flow inlet, where the pressure was specified as zero normal

gradient. A pressure outlet boundary condition was used, namely, the pressure was set as zero while u_x, u_y, and u_z were specified as zero normal gradient. A non-slip wall boundary condition was prescribed on the hull surface and slip boundary conditions were applied for the domain bottom and the two lateral walls. As the Froude numbers were small, the free surface effect can be ignored[17]. correspondingly, the free surface was treated as a symmetric boundary. This simplification thus ignored the heave, roll and pitch motions of the semi-submersible models.

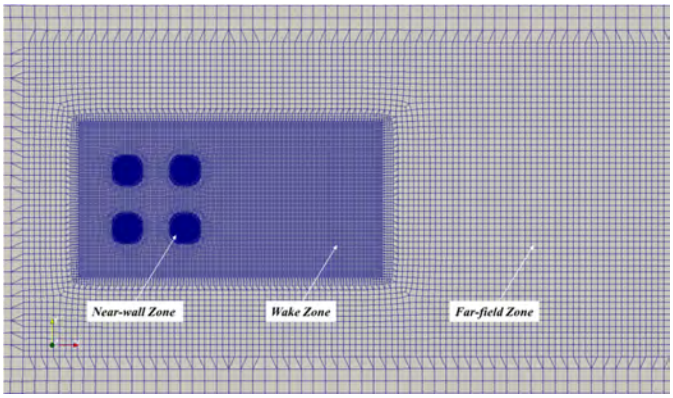

(a) Computational domain

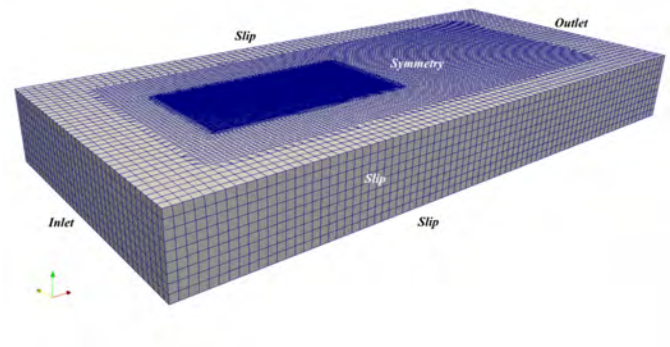

(b) boundary conditions

FIGURE 4. Computational domain and boundary conditions.

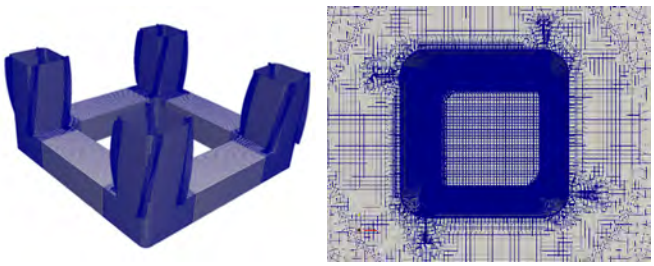

FIGURE 5. Details of the refinement zone around the semi-submersible and helical strakes.

The distribution of wall *y*+ values on the semi-submersible surface near the end of the solution time is shown in Figure 6. For the majority of the underwater portion, the wall *y*+ values range from about 1 to around 10, except in a very small range around the pontoon edge where they are locally higher, indicating sufficient resolution in the near boundary layer for the delay detached-eddy simulation (DDES).

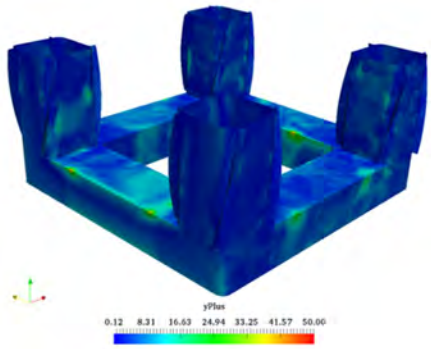

FIGURE 6. Distribution of wall *y*+ values on the surface of the semi-submersible, solution time at t=300s.

The semi-submersible can freely move in 3 degrees of freedom (3DOF), i.e. surge, sway and yaw. The semi-submersible is positioned in the uniform and constant inflow velocity field. And effects of the free water surface are assumed to be negligible and thus the water surface is taken into account as a symmetry boundary condition.

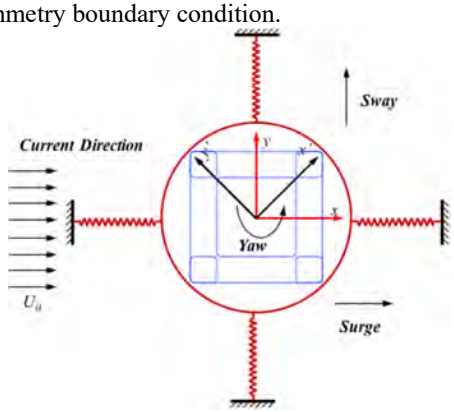

FIGURE 7. The distribution of linear springs system make how the semi-submersible freely move in 3 degrees of freedom (3DOF), i.e. surge, sway and yaw

Discretization format

The governing equations are discretized using a finite volume method for solving the incompressible Navier–Stokes equations using solver naoe-FOAM-SJTU. The time discretization is done using second order implicit Euler scheme. A second order Gauss integration is used for spatial gradient calculations. The convection operator is discretized using a total variation diminishing (TVD) scheme. The merged PISO-SIMPLE (PIMPLE) algorithm is used for solving the coupled pressure–velocity equations.

SST-DDES Model

In the present study, the separated flows past columns of semi-submersibles are very important to the VIM behavior. Therefore, in order to predict VIM responses accurately, an

improved RANS-LES hybrid model is required. The turbulent model is using the Shear Stress Transport (SST) based Delay Detached eddy simulation (DDES), which provides the accuracy of LES for highly separated flow regions and computational efficiency of RANS in the near-wall region, making it applicable to the simulation of VIM. In the SST-DDES turbulence model, the computed turbulent length scale is defined as:

$$l_{DDES} = l_{RANS} - f_d max(0, l_{RANS} - C_{DES}\Delta) \quad (2)$$

Where, $l_{RANS} = \frac{\sqrt{k}}{\beta^* \omega}$ is the RANS computed turbulent length scale; $\Delta = \sqrt[3]{V}$ is size of sub-grid;

$$C_{DES} = (1 - F_1){C_{DES}}^{k-\varepsilon} + F_1 {C_{DES}}^{k-\omega} \quad (3)$$

$$f_d = 1 - \tanh[(C_{d1} r_d)^{C_{d2}}] \quad (4)$$

$$r_d = \frac{v_t + v}{\kappa^2 {d_w}^2 \sqrt{0.5(S^2 + \Omega^2)}} 1 - \tanh[(C_{d1} r_d)^{C_{d2}}] \quad (5)$$

v_t, v are the eddy and molecular viscosities respectively, κ = 0.41 is the von-Kaman constant. d_w is the distance to wall. f_d is zero in the near wall boundary layer to deactivate the DES limiter and ensure that DES works in the RANS manner. C_{DES} is the DES constant which is 0.61, F_S can be F_1 or F_2, and F_2 is used in the paper of Zhao et al (2016). The suitability of the present SST-DDES model has been clarified by Zhao et al (2016) for solving flow past two circular cylinders in tandem. More about the SST-DDES model can also be seeing in Zhao's paper[18].

NUMERICAL RESULTS

Free Decay Tests

In order to confirm the accuracy of the simplified spring system in simulations, free decay tests in calm water for 0 degree of incident angle. The model tests were conducted in a towing tank and for the CFD simulations, the semi-submersible model was subjected to uniform incident current. For cross-flow and inline decay test, the platform is given with an initial velocity of 0.068m/s and allowed to freely oscillate. For the yaw decay test, the initial rotation speed is set as 0.5 rad/s.

Table 3 shows the natural periods for the CFD calculations in comparison with the Walls et al. (2007)[6] tests. The natural period of surge, sway and yaw motion for without strakes case is 14.9s, 23.3s and 5.5s, respectively. The natural period of surge, sway and yaw motion for with strakes case is 15.8s, 25.0s and 6.5s, respectively. As seen, the computed natural periods agree well with the experimental data and the maximum difference is around 10%. The natural periods of column without helical strakes (with round corner) is less than the experimental data of Walls et al. while data of semi-submersible with helical strakes is higher than the experimental data in natural periods.

TABLE 3. Natural periods from the calm water free decay tests for 0° current incidence.

Natural periods(s)	Direction	Wall(2007) (s) (R=0)	Present CFD(s) (R=0.031m)	Difference (%)
without strakes	Surge	15.7	14.9	5.10%
	Sway	24.4	23.3	4.51%
	Yaw	5.9	5.5	6.78%
with strakes	Surge	-	15.8	0.64%
	Sway	-	25.0	2.46%
	Yaw	-	6.5	10.16%

R denotes the round corner of columns.

Figure 8 shows the time history and Fourier transform result of free decay test for 0° current incidence.

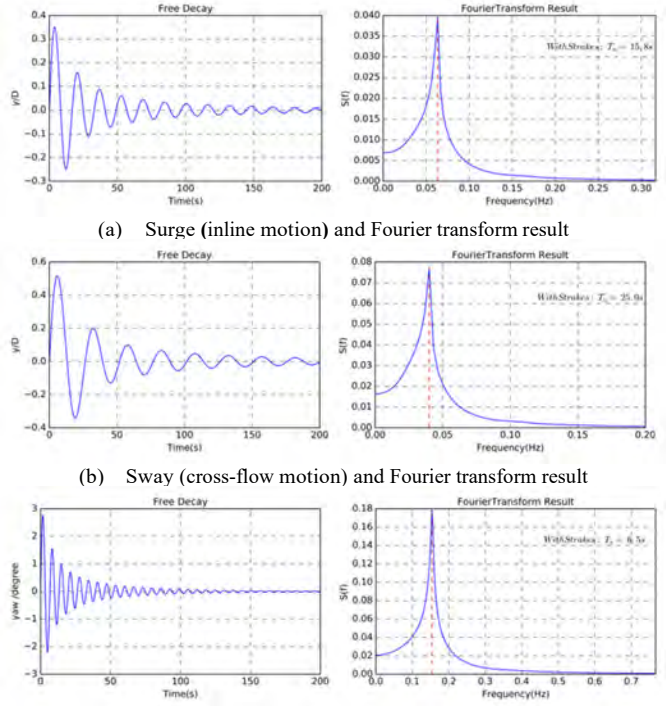

(a) Surge (inline motion) and Fourier transform result

(b) Sway (cross-flow motion) and Fourier transform result

(c) yaw and Fourier transform result

FIGURE 8. Time history and Fourier transform result of free decay test for 0° current incidence: (a) surge (inline motion), (b) sway (cross-flow motion), (c) yaw

VIM Responses and Motion Trajectory

Figure 9 shows the time histories of surge, sway and yaw motion for 0 incident angles at *Ur* = 8, *Ur* = 11 and *Ur* = 20, respectively. The inline and cross-flow motions are normalized by the column width *D*. As shown in Figure 8, for the case of without helical strakes the amplitudes of the sway motion at *Ur* = 20 are obviously larger than amplitudes at *Ur* = 8 and *Ur* = 11. When it comes to the case of with helical strakes, the increase of sway (cross-flow direction) motion amplitudes is not so obvious. Furthermore, with the increase of

reduced velocity, the surge (inline direction) motion displacement of the semi-submersible is increased significantly. In general, the computed result indicate that the VIM response of inline motion is much less than that of cross-flow motion. Table 4. is the summary of simulated VIM sway motion.

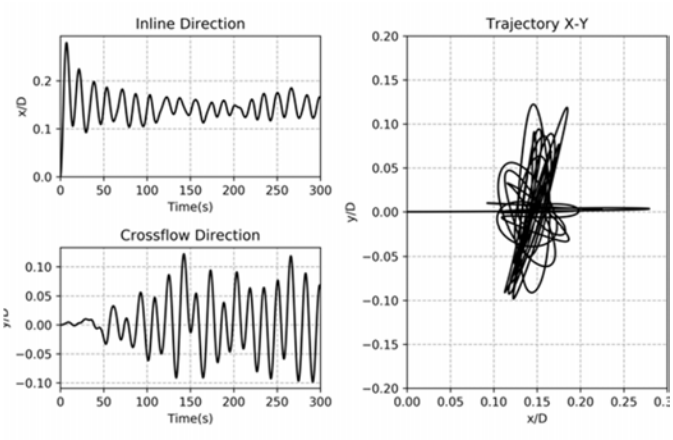

(a) without strakes U_r =8

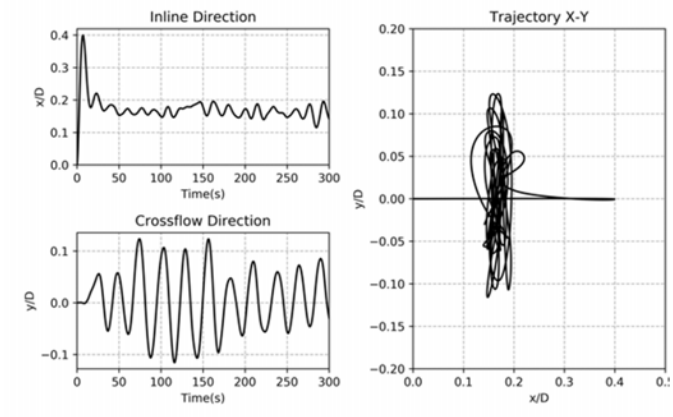

(b) with strakes U_r =8

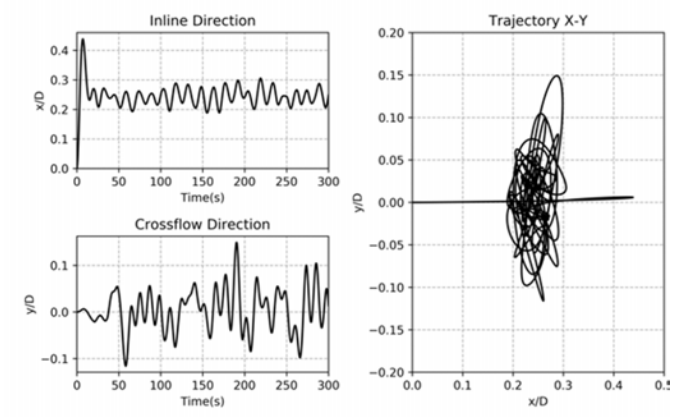

(c) without strakes U_r =11

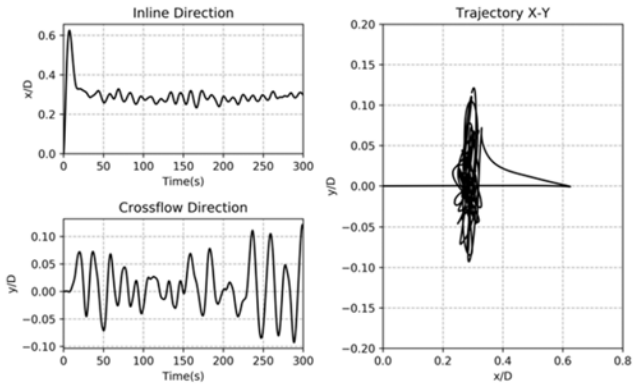

(d) with strakes U_r =11

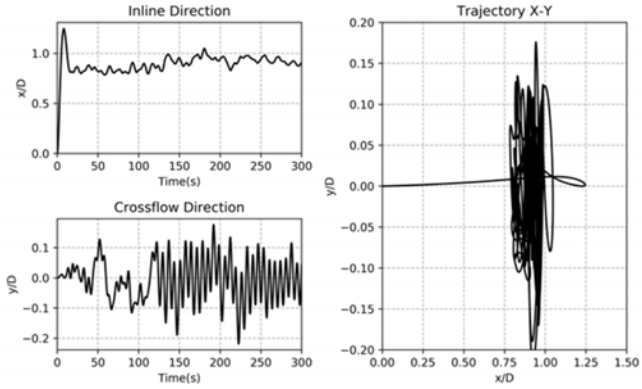

(e) without strakes U_r =20

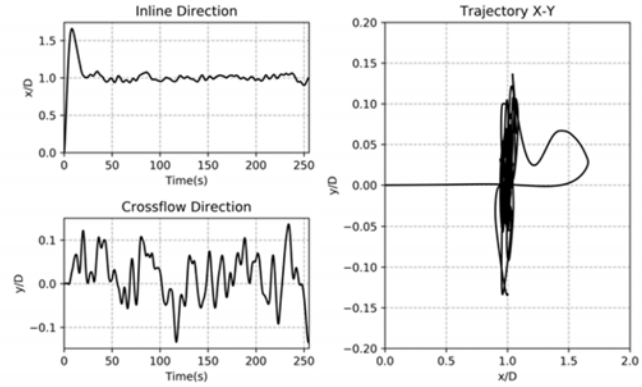

(f) with strakes U_r =20

FIGURE 9. Time history of VIM surge and sway motion and the motion trajectory for different reduced velocity

TABLE 4. Summary of the simulated VIM sway motion

Reduced velocity (U_r)	**without strakes**		**with strakes**	
	Sway period T_y	Sway max amplitude y/D	Sway period T_y	Sway max amplitude y/D
Ur =8	16.8	0.12	27.3	0.114
Ur =11	35.0	0.15	40.0	0.11
Ur =20	6.8	0.18	15.2	0.13

Effects of the helical strakes on VIM

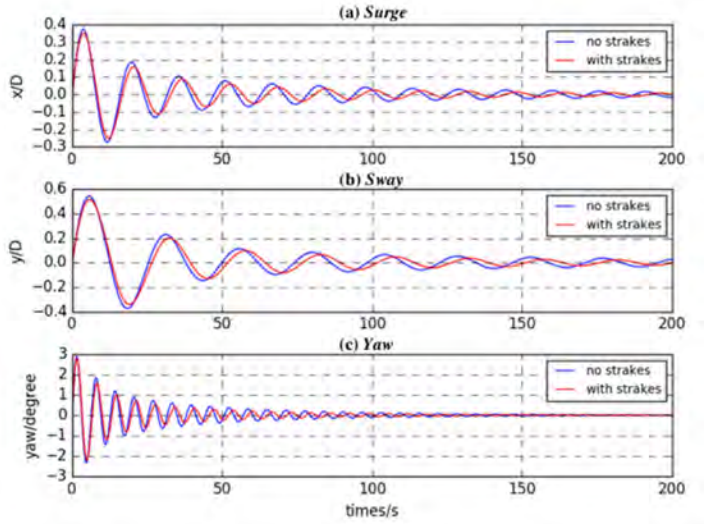

FIGURE 10. compare the time history of free decay test for 0° current incidence for with and without helical strakes

As show in Figure 10 and Table 3, compare the time history of free decay test for with and without helical strakes case, it is found that the helical strakes have an effect on the natural periods of semi-submersible. With the helical strakes, the natural periods of semi-submersible become a little higher.

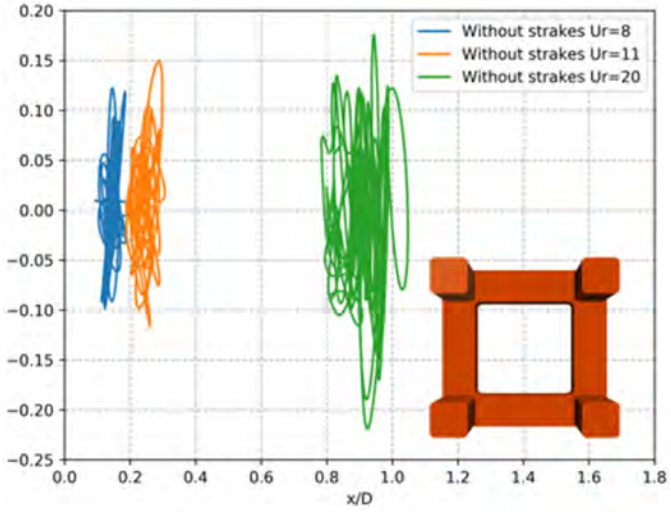

(a) VIM motion trajectory without strakes

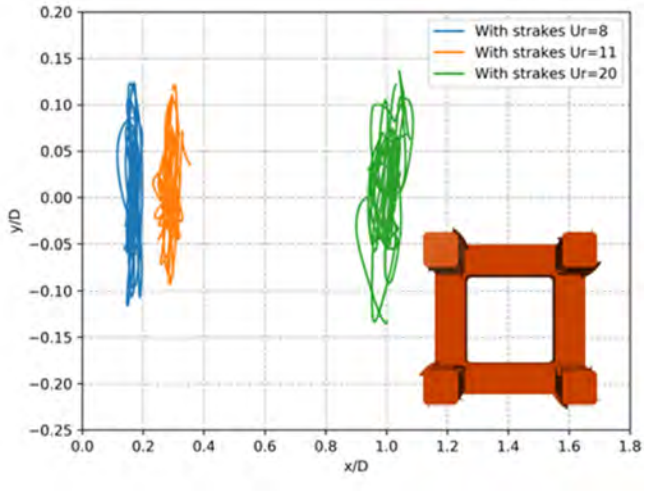

(b) VIM motion trajectory with strakes

FIGURE 11. compare of the VIM motion trajectory of semi-submersible platform with and without helical strakes (0° current incidence)

As shown in Figure 11, The amplitude of surge (inline direction) motion is a little increase by installing with strakes for different reduced velocity (*Ur*). When the reduced velocity *Ur*=20, the amplitudes have a big increase, from 0.9 to 1.0. While the sway (cross-flow direction) motion is the different case for with and without helical strakes. As shown in the figure 10, the amplitude of sway (cross-flow direction) motion is decreased by the helical strakes. In general, the helical strakes reduced the sway motion of semi-submersible.

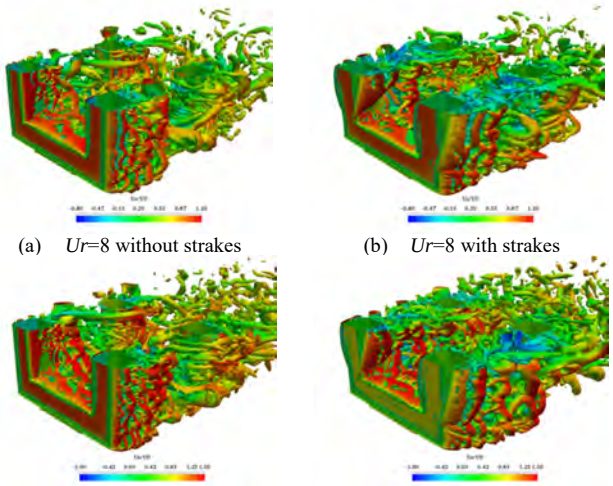

(a) *Ur*=8 without strakes (b) *Ur*=8 with strakes

(c) *Ur*=11 without strakes (d) *Ur*=11 with strakes

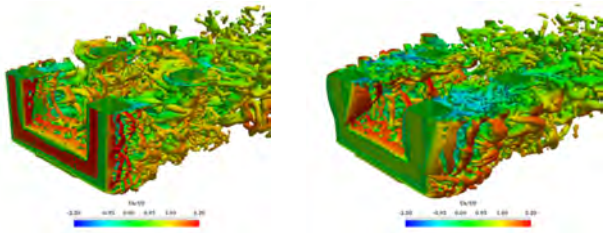

(e) *Ur*=20 without strakes (f) *Ur*=20 with strakes

FIGURE 12. Tail vortex structure of semi-submersible platform with Q =5, dye visualization with x-direction non-dimensioned velocity magnitude (0° current incidences)

Figure 12 is iso-surface contour of the second invariant of the velocity gradient tensor Q colored with x-direction non-dimensioned velocity magnitude. There is a difference between vortex structures for semi-submersible installed with and without helical strakes. For the case of without strakes, the vortexes are generated as they follow the curvature of the rounded corner and are shed. The helical strakes are to disrupt this shedding and allow for the flow to separate differently through the height of the column. With the helical strakes, we could found that the vortexes are generated are shed from the strakes' edge.

Vorticity Contours

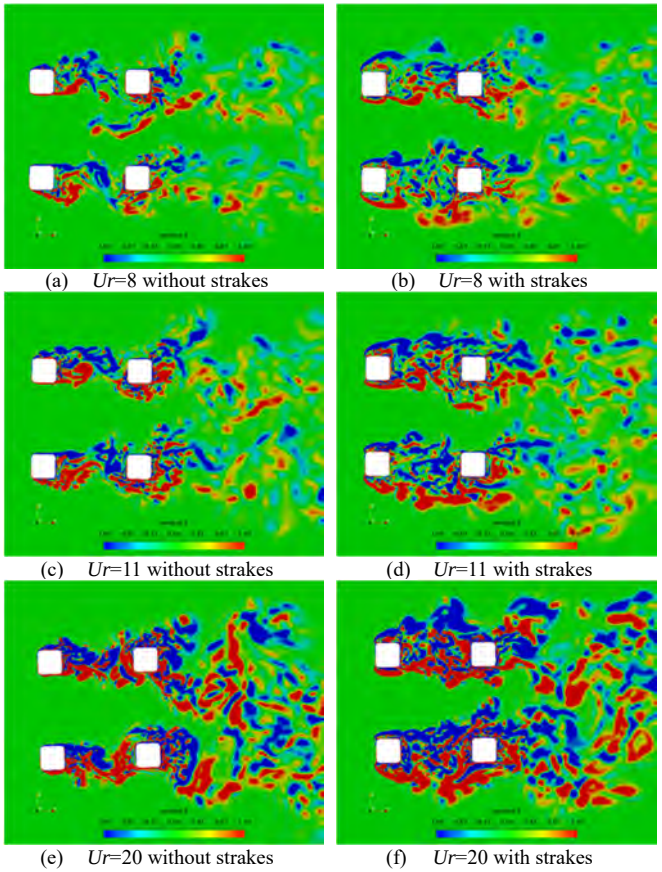

(a) *Ur*=8 without strakes (b) *Ur*=8 with strakes

(c) *Ur*=11 without strakes (d) *Ur*=11 with strakes

(e) *Ur*=20 without strakes (f) *Ur*=20 with strakes

FIGURE 13. Distribution of vorticity contour on the z/L=0.5 horizontal plane near middle column with different reduced velocity (Ur) (0° heading)

Figure. 13 shows the vorticity contour on the z/L=0.5 horizontal plane near middle column with different reduced velocity (Ur =8, 11, 20). It can be seen that strong vortexes are generated behind the upstream columns. The vortex distribution of upstream region has been changed by the downstream columns stand in the wake area. Compare the contours of vorticity between with and without helical strakes, The upstream columns therefore show a slightly weaker vortex strength due to the effect of helical strakes.

CONCLUSIONS

In this study, CFD calculations for a semi-submersible model with and without helical strakes have been presented. To carry out the calculations, the shear stress transport based delay detached eddy simulation (SST-DDES) model has been adopted to simulate the VIM of the deep draft semi-submersible for three distinct current speeds. Compared with natural periods, it is found that the present results agree well with the Walls et al. (2007) experimental data, which prove our CFD solver naoe-FOAM-SJTU is applicable and reliable to study VIM of semi-submersible. The computed results indicate that the VIM response of inline motion is much less than that of cross-flow motion. It is found that the amplitude of surge (inline direction) motion is a little increased by installing strakes for all the reduced velocity (Ur). While the amplitude of sway (cross-flow direction) motion is decreased by the helical strakes. In general, the helical strakes reduced the sway motion of semi-submersible. In this study, we didn't investigate the influence of different current headings which can cause lock-in, potentially resulting in large and extreme motion responses. The influence of different current headings is also worth investigating. The work of more systematic tests will need to be carried out in my future work.

ACKNOWLEDGMENTS

This work is supported by the National Natural Science Foundation of China (51490675, 11432009, 51579145), Chang Jiang Scholars Program (T2014099), Shanghai Excellent Academic Leaders Program (17XD1402300), Program for Professor of Special Appointment (Eastern Scholar) at Shanghai Institutions of Higher Learning (2013022), Innovative Special Project of Numerical Tank of Ministry of Industry and Information Technology of China (2016-23/09) and Lloyd's Register Foundation for doctoral student, to which the authors are most grateful..

REFERENCES

[1] Liu, M., Xiao, L., Kou, Y., and Lu, H., 2017, "Numerical Study on Vortex-Induced Motions of Semi-Submersibles

With Various Types of Columns," *Volume 7A: Ocean Engineering*, ASME, p. V07AT06A070.

[2] Chen, C.-R., and Chen, H.-C., 2015, "CFD Simulation of Vortex-Induced Motions of a Deep Draft Semi-Submersible Platform," *Proceedings of the Twenty-Fifth (2015) International Ocean and Polar Engineering Conference*, Kona, Big Island, Hawaii, USA, pp. 1071–1078.

[3] Xiang, S., Cao, P., Rijken, O., Ma, J., and Chen, Y., 2010, "Riser VIM Fatigue Design Induced by Deep Draft Semi-Submersible," *29th International Conference on Ocean, Offshore and Arctic Engineering: Volume 5, Parts A and B*, ASME, pp. 365–374.

[4] Kara, M. C., Kaufmann, J., Gordon, R., Sharma, P. P., and Lu, J. Y., 2016, "Application of CFD for Computing VIM of Floating Structures," *Offshore Technology Conference*, Offshore Technology Conference, pp. 2–5.

[5] Rijken, O., 2014, "Examining the Effects of Scale, Mass Ratios and Column Shapes on the Vortex Induced Motion Response of a Semisubmersible Through CFD Analyses," *Volume 2: CFD and VIV*, ASME, p. V002T08A028.

[6] Waals, O. J., Phadke, A. C., and Bultema, S., 2007, "Flow Induced Motions on Multi Column Floaters," *Volume 1: Offshore Technology; Special Symposium on Ocean Measurements and Their Influence on Design*, ASME, pp. 669–678.

[7] Gonçalves, R. T., Rosetti, G. F., Fujarra, A. L. C., and Oliveira, A. C., 2012, "Experimental Study on Vortex-Induced Motions of a Semi-Submersible Platform with Four Square Columns, Part I: Effects of Current Incidence Angle and Hull Appendages," Ocean Eng., **54**, pp. 150–169.

[8] Gonçalves, R. T., Rosetti, G. F., Fujarra, A. L. C. A. L. C. A. L. C., Oliveira, A. C., Gon??alves, R. T., Rosetti, G. F., Fujarra, A. L. C. A. L. C. A. L. C., and Oliveira, A. C., 2013, "Experimental Study on Vortex-Induced Motions of a Semi-Submersible Platform with Four Square Columns, Part II: Effects of Surface Waves, External Damping and Draft Condition," Ocean Eng., **62**, pp. 10–24.

[9] Chen, C.-R., and Chen, H.-C., 2016, "Simulation of Vortex-Induced Motions of a Deep Draft Semi-Submersible in Current," Ocean Eng., **118**, pp. 107–116.

[10] Antony, A., Vinayan, V., Holmes, S., Spernjak, D., Kim, S. J., and Halkyard, J., 2015, "VIM Study for Deep Draft Column Stabilized Floaters," *Offshore Technology Conference*, Offshore Technology Conference, pp. 1–16.

[11] Zhou, T., Razali, S. F. M., Hao, Z., and Cheng, L., 2011, "On the Study of Vortex-Induced Vibration of a Cylinder with Helical Strakes," J. Fluids Struct., **27**(7), pp. 903–917.

[12] Ranjith, E. R., Sunil, A. S., and Pauly, L., 2016, "Analysis of Flow over a Circular Cylinder Fitted with Helical Strakes," Procedia Technol., **24**, pp. 452–460.

[13] Holland, V., Tezdogan, T., and Oguz, E., 2017, "Full-Scale CFD Investigations of Helical Strakes as a Means of Reducing the Vortex Induced Forces on a Semi-Submersible," Ocean Eng., **137**(April), pp. 338–351.

[14] Xu, Q., Kim, J., Bhaumik, T., O'Sullivan, J., and Ermon, J., 2012, "Validation of HVS Semisubmersible VIM Performance by Model Test and CFD," *Volume 1: Offshore Technology*, ASME, p. 175.

[15] Kim, J., Magee, A., Yeoh, K., and Guan, H., 2012, "CFD Simulation of Flow-Induced Motions of a Multi-Column Floating Platform," PETROMIN - Asia´s Explot. Prod. Bus. Mag., pp. 44–52.

[16] Tan, J. H. C., Magee, A., Kim, J. W., Teng, Y. J., and Ahmad Zukni, N., 2013, "CFD Simulation for Vortex Induced Motions of a Multi-Column Floating Platform," *Volume 7: CFD and VIV*, ASME, p. V007T08A066.

[17] Liu, M., Xiao, L., Yang, J., Tian, X., Liu, M., Xiao, L., Yang, J., and Tian, X., 2017, "Parametric Study on the Vortex-Induced Motions of Semi-Submersibles : Effect of Rounded Ratios of the Column and Pontoon Parametric Study on the Vortex-Induced Motions of Semi-Submersibles : Effect of Rounded Ratios of the Column and Pontoon," Phys. Fluids, **29**(5), pp. 55101–19.

[18] Weiwen Zhao and Decheng Wan. 2016, "Detached-Eddy Simulation of Flow Past Tandem Cylinders," Appl. Math. Mech., **37**(12), pp. 1272–1281.